CORA Cork Open Research Archive
Cartlann Taighde Oscailte Chorcaí

Title	Excitable interplay between lasing quantum dot states
Authors	Dillane, Michael;Dubinkin, I.;Fedorov, N.;Erneux, T.;Goulding, D.;Kelleher, Bryan;Viktorov, E. A.
Publication date	2019-07-17
Original Citation	Dillane, M., Dubinkin, I., Fedorov, N., Erneux, T., Goulding, D., Kelleher, B. and Viktorov, E. A. (2019) 'Excitable interplay between lasing quantum dot states', Physical Review E, 100(1), 012202 (6pp). doi: 10.1103/PhysRevE.100.012202
Type of publication	Article (peer-reviewed)
Link to publisher's version	https://link.aps.org/doi/10.1103/PhysRevE.100.012202 - 10.1103/PhysRevE.100.012202
Rights	© 2019, American Physical Society. All rights reserved.
Download date	2026-10-30 10:36:59
Item downloaded from	https://hdl.handle.net/10468/8520

UCC
University College Cork, Ireland
Coláiste na hOllscoile Corcaigh

Excitable interplay between lasing quantum dot states

M. Dillane,[1,2] I. Dubinkin,[3] N. Fedorov,[3] T. Erneux,[4] D. Goulding,[2,5,6] B. Kelleher,[1,2] and E. A. Viktorov[3]
[1]*Department of Physics, University College Cork, Cork, Ireland*
[2]*Tyndall National Institute, University College Cork, Lee Maltings, Dyke Parade, Cork, Ireland*
[3]*National Research University of Information Technologies, Mechanics and Optics, Saint Petersburg, Russia*
[4]*Optique Nonlinéaire Théorique, Campus Plaine, CP 231, 1050 Bruxelles, Belgium*
[5]*Centre for Advanced Photonics and Process Analysis, Cork Institute of Technology, Cork, Ireland*
[6]*Department of Mathematics, Cork Institute of Technology, Cork, Ireland*

(Received 16 October 2018; published 17 July 2019)

The optically injected semiconductor laser system has proven to be an excellent source of experimental nonlinear dynamics, particularly regarding the generation of excitable pulses. Typically for low-injection strengths, these pulses are the result of a small above-threshold perturbation of a stable steady state, the underlying physics is well described by the Adler phase equation, and each laser intensity pulse is accompanied by a 2π phase rotation. In this article, we show how, with a dual-state quantum dot laser, a variation of type I excitability is possible that cannot be described by the Adler model. The laser is operated so that emission is from the excited state only. The ground state can be activated and phase locked to the master laser via optical injection while the excited state is completely suppressed. Close to the phase-locking boundary, a region of ground-state emission dropouts correlated to excited-state pulses can be observed. We show that the phase of the ground state undergoes bounded rotations due to interactions with the excited state. We analyze the system both experimentally and numerically and find excellent agreement. Particular attention is devoted to the bifurcation conditions needed for an excitable pulse as well as its time evolution.

DOI: 10.1103/PhysRevE.100.012202

I. INTRODUCTION

Noise-induced and perturbed dynamics attract significant interest in complex nonlinear systems. One of the most important noise-induced effects, ubiquitous in systems of coupled oscillators, is excitability. Excitable events were originally studied and classified in the neural sciences [1] and have since been observed in other biological settings including cardiac arrhythmia [2], chemical reactions [3–5], and most pertinently for this work, in many laser systems [6–13]. Recently, there has been a growing interest in advancing optical information processing outside conventional binary schemes, particularly using photonic and optoelectronic systems to mimic neural networks for computing (see Ref. [14] and the references therein). In several schemes, a laser acts as an artificial neuron with excitable pulses mimicking neural spikes, combining essential processing tasks of logic-level restoration, cascadability, pattern detection, and recurrent memory [14–19].

In this article, we are concerned with the optically injected laser system [20]. In the limit of weak injection and small detuning, the first-order Adler phase equation can be derived from the full laser equations [21]. The phase locking arises via a saddle-node bifurcation coinciding with a homoclinic bifurcation (SNH) [otherwise known as a saddle-node infinite period bifurcation (SNIPER) or saddle node on an infinite cycle (SNIC)]. Close to the phase-locking boundary, perturbations can kick the system from the stable steady state (the node) beyond the unstable saddle point to yield a 2π phase rotation accompanied by an intensity pulse [20,22]. Such excitable events are classified as type I excitability [23]. Depending on the laser type, different variations of responses are possible, including single and multipulse excitability [6–8]. Furthermore, perturbations yielding an excitable pulse can be noise induced [8,22] or deterministic [24,25].

When undergoing optical injection, InAs-based quantum dot (QD) lasers exhibit significantly larger and more controllable regions of excitability compared to conventional semiconductor lasers. This is mainly due to the highly damped relaxation oscillations of QD lasers. Another distinguishing characteristic of QD lasers is the propensity to lase from multiple distinct energy states: Depending on device and operating parameters, emission may come from the ground state (GS) only, from the first excited state (ES) only, or simultaneously from both states [26,27]. The behavior of such devices while emitting from the GS only has been well investigated in recent years and studies of the behavior under optical injection have revealed many interesting phenomena [28–30]. While studies of optically injected QD lasers in the two-state or the ES-only regimes are much more rare, interest in these regimes has recently grown and particularly in the case where the free-running operation is ES lasing only and the GS is injected. Of note for this configuration is an ultrafast all-optical switching between the GS and ES found in Ref. [31], and an all-optical gating effect when the injected and saturable GS operates as a gate for the ES output [32]. Enhanced stability has also been predicted numerically, suggesting many potentially useful applications [33]. The mechanism behind this dual lasing phenomenon results from the cascadelike relaxation pathway for the carriers in the dot: The

 ©2019 American Physical Society

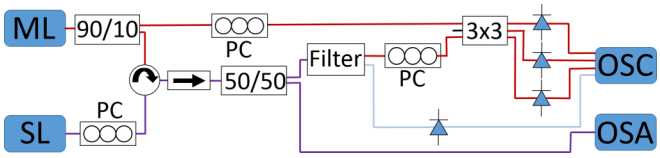


FIG. 1. Setup for unidirectional injection experiment where the slave laser (SL) is a QD laser and the master laser (ML) is a tunable laser source (TLS). PC is the polarization controller, OSC is the oscilloscope, and OSA is the optical spectrum analyzer. The red lines represent light at approximately 1300 nm close to the GS emission, the blue is ES only, and the purple is both GS and ES.

carriers are first captured from the wetting layer by the ES and subsequently relax into the GS. Therefore, the lasing states in a QD laser can be considered as coupled oscillators with strongly asymmetric nonlinear coupling due to the cascadelike pathway for the carriers. Antiphase dynamics appear in cases such as Ref. [18] where the GS intensity is in antiphase with the ES intensity. Similar antiphase behavior has been observed in semiconductor ring lasers when the two directional modes operate in antiphase [13].

We experimentally and theoretically analyze optically injected QD lasers when the free-running operation is lasing from the ES only. We optically inject the GS and find a SNH bifurcation at low-injection levels. Noise-induced excitable ES intensity pulsations and corresponding antiphase GS intensity dropouts are obtained close to this phase-locking boundary. These antiphase excitable events display type I excitability characteristics. We show that the asymmetric cascadelike coupling leads to excitable events built on an itineracy of unstable lasing states. By measuring the phase of the GS during an excitable event, we find that 2π phase slips are not obtained, and thus the excitable response cannot be explained by the Adler equation [34]. This is in sharp contrast to all existing reports on low-injection excitability. Bounded phase phenomena are possible for the optical injection system but have typically been associated with Hopf bifurcations [35,36]. In contrast, here the dual-state property of our QD lasers allows bounded phase excitable pulses near the SNH bifurcation.

II. EXPERIMENT

The device used is a 300-μm-long, InAs/GaAs QD laser similar to that used in Ref. [31]. At 20 °C, the GS threshold is 32 mA. A dual-state lasing regime exists between 57 and 72 mA where emission is obtained from both the GS (at ∼1300 nm) and the ES (at ∼1215 nm). For pump currents greater than 72 mA, the GS is completely suppressed and only ES light is emitted (the ES emission is more than 30 dB higher than that from the GS). For this experiment the laser is pumped at 73 mA. A schematic of the experimental setup is shown in Fig. 1. The laser emits on a single longitudinal mode from the GS while the ES emission is from many longitudinal modes. The QD laser is optically injected with light from a master laser (ML)—an Agilent 81672B tunable laser source (TLS)—with a linewidth of approximately 100 kHz and a minimum step increment of 0.1 pm. Here, 10% of the ML light is used for a phase measurement (see below). The

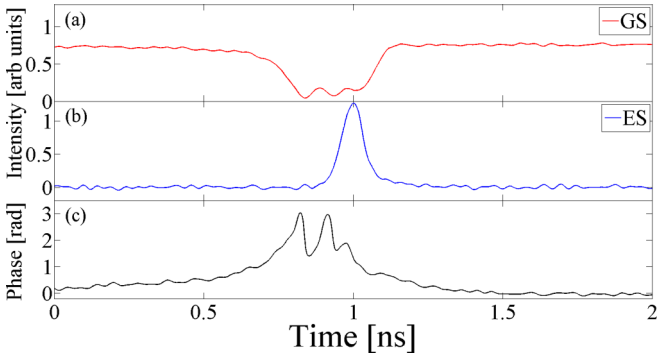


FIG. 2. Time trace of excitability. (a) shows the 300-ps dropout, (b) shows the 80-ps ES pulse, and (c) is the phase. Detuning is −8 GHz.

remaining 90% goes through a circulator and is injected into the QD slave laser (SL). A polarization controller maximizes the coupling between the ML and the QD laser. The output from the injected slave is split, with 50% used for the phase measurement (described below) and 50% for detuning measurements. In the conventional injection system the detuning is easily determined. However, for the control parameters used in this system, the GS is subthreshold when the QD laser is free running. Nonetheless, while the GS mode is suppressed by more than 30 dB without optical injection, it is still visible due to amplified spontaneous emission. We define zero detuning to be at the peak of this subthreshold mode.

The two control parameters are the injection strength controlled by the ML power and the detuning controlled by the ML wavelength. Initially the QD laser is free running and emitting from the ES only. By injecting into the GS with sufficient strength, phase locking occurs and the GS can be made to lase with the ES suppressed by 39.7 dB relative to its free-running value. As the frequency of the master laser is decreased toward the unlocking boundary, deep GS intensity dropouts are observed. Experimental measurements of the intensities are shown for approximately −8 GHz detuning in Fig. 2. The GS dropouts have widths of approximately 300 ps and the minimum intensity is close to zero. These dropouts have corresponding large pulsations in the ES achievable due to the gain available during the dropout. The ES pulses are much shorter with a full width at half maximum (FWHM) of approximately 80 ps. We interpret the behavior as antiphase, dual-state excitability.

Using the phase-resolving technique of Ref. [37], we can analyze the phase behavior of the GS. In the injected system, it involves the use of a 3×3 coupler with one input coming from the ML (the 10% mentioned above) and one from the SL (the 50% mentioned above). The other input is left empty (see Fig. 1). By simultaneously measuring the three outputs of the coupler one can find the real-time phase evolution. For the conventional one-state injection system where only the ground state is involved, 2π phase rotations (or multiples thereof) are observed for each excitable event [6,22]. In the dual-state system of this work, however, this is not the case and we observe bounded phase trajectories as shown in Fig. 2(c). Figure 3 shows the phase evolution in a two-dimensional projection onto the electric field plane.

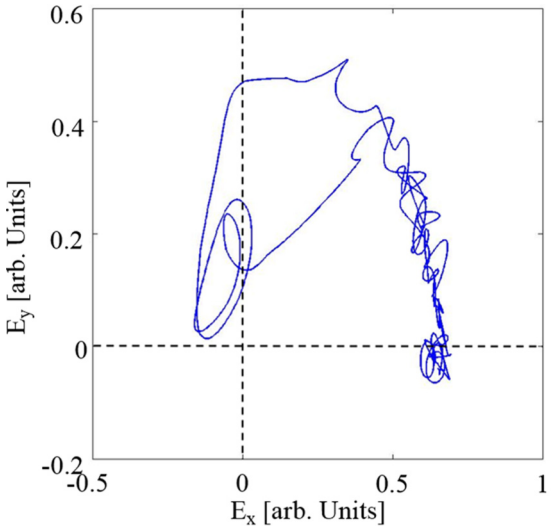


FIG. 3. Real and imaginary parts of the electric field showing the phase evolution. The steady state is at approximately (0.6,0). When noise triggers a pulse it results in a bounded trajectory that does not go around the origin. The spiral close to the origin suggests the presence of a saddle focus.

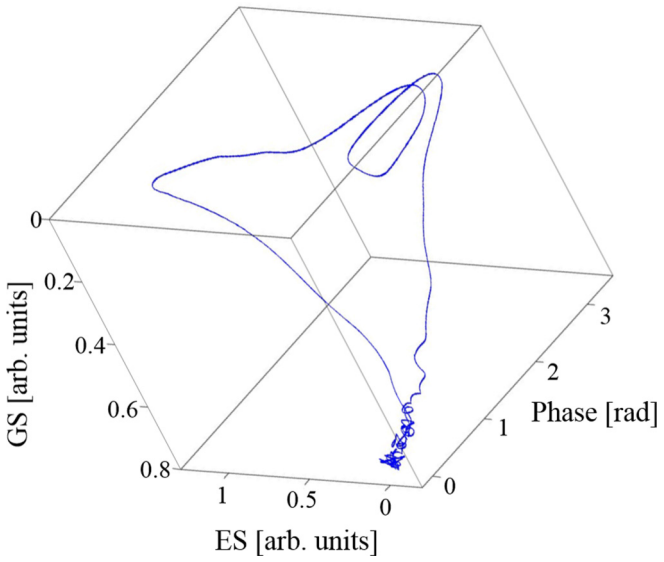


FIG. 4. A three-dimensional figure showing the phase and the GS and ES intensities. When the ES turns on, it pulls the phase away from the origin, stopping a 2π rotation. The saddle focus has two oscillations as in Fig. 3 but it is not visible from this reference angle.

This bounded phase trajectory cannot be explained by the simple Adler equation. Moreover, the presence of spiralling oscillations is also visible. They correspond to the ringing in the lower plateau of the dropout in Fig. 2(a) and in the upper part of the phase trajectory in Fig. 2(c). This ringing can be identified as a form of relaxation oscillation (RO) and is evocative of the turn-off transient for the underlying off-state for the GS in the free-running configuration, itself a focus point. The ringing should not be identified with the relaxation oscillations of the free-running laser emitting from the ES only. The ringing is also visible in the three-dimensional plot of the phase and the intensities of the GS and ES shown in Fig. 4.

We ascribe the bounded GS phase to the presence of the ES pulse and the interstate phase-amplitude coupling arising from inhomogeneous broadening due to the quantum dot size distribution. This phenomenon has been shown to play an important role in the system, leading to hysteresis with control parameter variation [38].

We note that in Ref. [39] pulses could be created without accompanying 2π rotations. This is very different from the case presented here. First, Ref. [39] considers a mutually coupled system where the presence of delay coupling allows for the generation of pulse trains rather than individual excitable pulses. Further, the pulse generating the train in Ref. [39] always arises from a 2π slip: It is only subsequent pulses in the train that might not involve a full slip. What is more, the influence of noise is also crucial in determining whether or not a 2π slip arises in Ref. [39]. In this work, the bounded rotation is deterministically induced by the inherent coupling of the ES and GS.

III. MODEL

To reveal the central feature of the dual-state excitable dynamics, we consider rate equations appropriate for our QD laser system [38] . They consist of equations for the complex electric field of the GS (E_g), the intensity of the ES (I_e), the occupation probabilities of the GS (n^g) and ES (n^e), and the carrier density in the wetting layer (n^w). We assume a cascadelike [wetting layer (WL)-ES-GS] relaxation pathway for the carriers in the dot as suggested in Ref. [26]. Since the equation for electric field of the GS (E_g) is complex, the phase space is nine dimensional,

$$\dot{E}_g = \tfrac{1}{2}\{(1+i\alpha)\big[2g_0^g\big(n_e^g+n_h^g-1\big)-1\big] + i4\beta g_0^e\big(n_e^e+n_h^e-1\big)\}E_g - i\Delta(t)E_g + \varepsilon, \quad (1)$$

$$\dot{I}_e = \big[4g_0^e\big(n_e^e+n_h^e-1\big)-1\big]I_e, \quad (2)$$

$$\dot{n}_{e,h}^g = \eta\big[2B_{e,h}n_{e,h}^e\big(1-n_{e,h}^g\big) - 2C_{e,h}n_{e,h}^g\big(1-n_{e,h}^e\big) - n_e^g n_h^g - g_0^g\big(n_e^g+n_h^g-1\big)|E_g|^2\big], \quad (3)$$

$$\dot{n}_{e,h}^e = \eta\big[-B_{e,h}n_{e,h}^e\big(1-n_{e,h}^g\big) + C_{e,h}n_{e,h}^g\big(1-n_{e,h}^e\big) + B_{e,h}^w n_{e,h}^w\big(1-n_{e,h}^e\big) - C_{e,h}^w n_{e,h}^e - n_e^e n_h^e - g_0^e\big(n_e^e+n_h^e-1\big)I_e\big], \quad (4)$$

$$\dot{n}_{e,h}^w = \eta\big[J - n_e^w n_h^w - 4B_{e,h}^w n_{e,h}^w\big(1-n_{e,h}^e\big) + 4C_{e,h}^w n_{e,h}^e\big]. \quad (5)$$

The subscripts e and h stand for electron and hole, respectively. The dots indicate differentiation with respect to $t = \tilde{t}/\tau_{\rm ph}$, where $\tilde{t}$ is time and $\tau_{\rm ph}$ is the photon lifetime. $\eta = \tau_{\rm ph}/\tau$, where τ denotes the carrier recombination time. J is the pump current, and the terms $B_{e,h}$ and $B_{e,h}^w$ are the capture rates to the GS and ES, respectively. The escape rates are given by the C terms and are linked to the capture rates B via the Kramers relation, as described in Ref. [38]. α is the usual GS linewidth enhancement factor. It is well known that a full treatment of this quantity in QD systems involves subtle details [40]. However, for simplicity, we treat it as a constant here and find that this is sufficient to analyze the

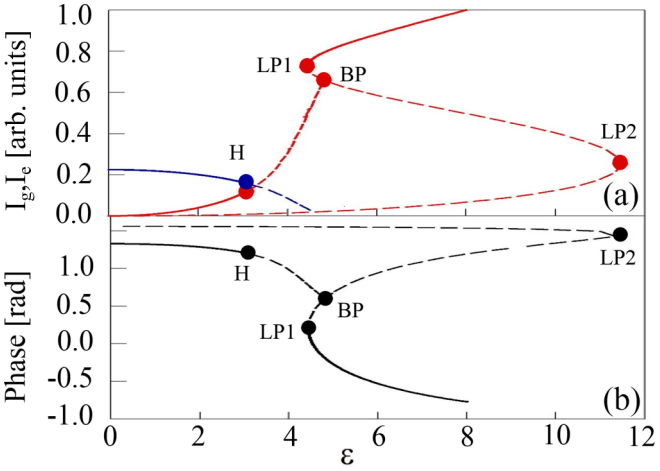


FIG. 5. Numerical bifurcation diagram. (a) shows the GS (red) and ES (blue) intensities vs ε. (b) shows the phase of the GS vs ε. Continuous (dashed) lines correspond to stable (unstable) branches. LP and H denote limit points and Hopf bifurcation points, respectively. BP denotes an unstable bifurcation point. LP1 denotes a saddle-node homoclinic (SNH) bifurcation and arises at $\varepsilon = 4.4373$. The fixed parameters are $\eta = 0.01$, $\Delta = 0$, $\alpha = 3$, $\beta = 2.4$, $g_0^g = g_0^e = 0.55$, $J = 56$, $B_{e,h} = B_{e,h}^w = 100$, $C_e^w = 0$, $C_h^w = 10^2$, $C_e = B_e \exp(-2)$, $C_h = B_h$. I_g is normalized by its value ($I_g = 223.83$) at $\varepsilon = 8$.

physics of the system. g^g and g^e are gain coefficients, β models the effect of inhomogeneous broadening [29,38], ε is the injection strength, and $\Delta = \omega_i - \omega_g$ is the detuning between the frequency of the injected light and that of the GS. The model takes into account the differing spin degeneracies in the QD energy levels, Pauli blocking, and interstate captures and escapes. Our two primary control parameters are the injection strength ε and the detuning Δ.

The bifurcation diagrams of the steady-state solutions are shown in Fig. 5. The point at which phase locking of the GS is achieved is that labeled LP1 at $\varepsilon = 4.4373$ and it is an SNH point. By injecting from the ML into the GS with $\varepsilon > 4.4373$, we find steady lasing from the GS with the ES suppressed. By progressively decreasing ε, there is a gradual decrease of the GS intensity while the ES remains off. As ε is further decreased below 4.4373, the system exhibits a cycle that emerges from a homoclinic loop at the limit point of the GS branches. This cycle manifests via GS dropouts and corresponding ES pulses and it disappears at the Hopf bifurcation H. The presence of the homoclinic bifurcation at the limit point means that at the onset of the pulsing, the repetition rate is arbitrarily low, confirming the type I characteristics of the phenomenon.

To include the effect of noise, a stochastic term $\sqrt{D}\xi(t)$ is added to Eq. (1) where $\xi(t)$ is a Gaussian white noise term and D is a constant. Then, close to LP1 but still in the phase-locked region, trains of noise-induced GS dropouts with corresponding ES pulses can be obtained. Figure 6 shows the evolution of both the GS and ES intensities and the GS phase for $\varepsilon = 4.4$. Figure 7 shows 3D plots of one noise-induced excitation at the same ε. All of these plots clearly show a ringing in the GS during the dropout. This is also clear in the experiment. This ringing results from a unique feature in this system: the

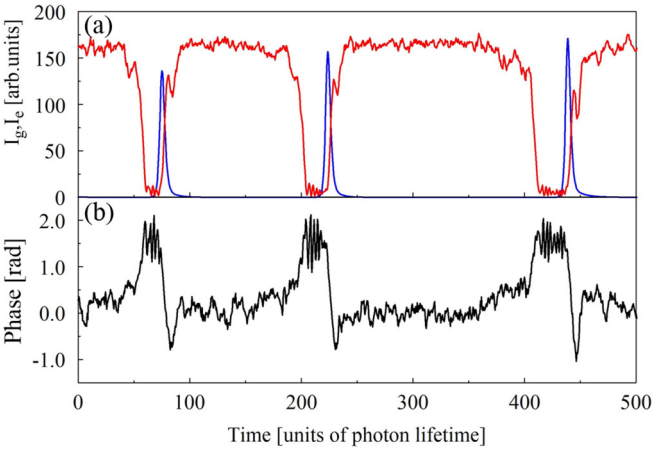


FIG. 6. Numerically obtained noise ($D = 0.25$) induced excitable events. (a) shows the GS (blue) and ES (red) intensities. (b) shows the corresponding phase evolution. The parameters are the same as in Fig. 5, where the vertical line indicates the point of operation.

presence of a saddle focus on the lower unstable branch in the bifurcation diagram as shown in Fig. 8 which is a zoom of Fig. 5(b). The excitable trajectory for the GS involves an attraction to this saddle focus with accompanying small-amplitude oscillations. In practice, the number of oscillations depends on the noise and can be small if the noise level is large as is clear from Fig. 6 and the 3D diagrams for different levels of noise shown in Fig. 7. Eventually the system hits the saddle focus and is kicked along the repulsive trajectory. This results in the observed large-amplitude ES pulsation which in turn affects the GS phase dynamics due to the inhomogeneous broadening-induced phase-amplitude coupling β. As with the experiment, the phase of the GS laser field is bounded in contrast to the unbounded phase of the Adler system. Thus, while the initial excitable trajectory arises as usual with the passing of the saddle created in the SNH bifurcation, the ensuing trajectory involves a passage through a saddle focus yielding both the ES pulse and the bounded phase GS cycle.

It is instructive to consider the ES excitation itself. Within the phase-locked region the steady-state behavior is GS on and ES off. The switching on of the ES during the excitable trajectory is similar to a Q-switched event. (This analogy was previously described in Ref. [38] where periodic trains were reported.) The very short ES pulses are excitable and thus could be used for pulse reshaping by feeding back some of the output into the device. Indeed,

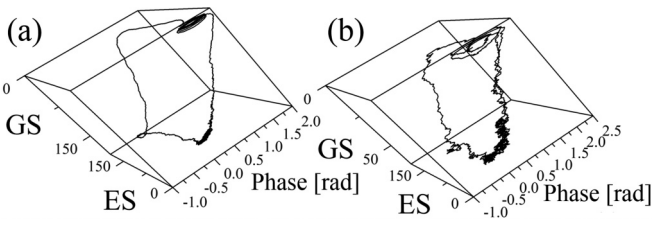


FIG. 7. Simulated 3D plots. (a) has a low-noise ($D = 0.25$) level and consequently displays many rotations in the spiral. (b) has a more realistic noise level ($D = 1$) and is in close agreement with the experimental results in Fig. 4.

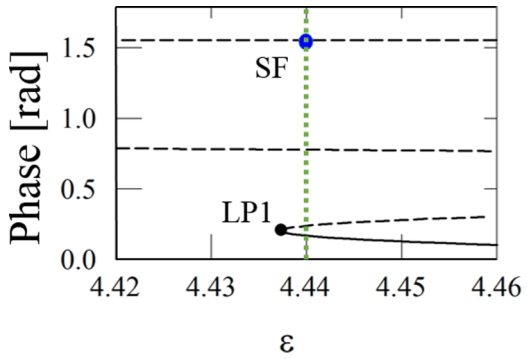


FIG. 8. Zoom of Fig. 5(b), where LP1 denotes the limit point which is a SNH bifurcation. The blue dot labeled SF represents the saddle focus. The green dotted line marks the operating injection strength where the noise induced events in Figs. 6 and 7 are found. The dashed lines are unstable branches and the solid lines are stable. The same operating parameters described in Fig. 6 are used here.

tunable pulse trains could be achieved in such a configuration. (Tunability outside the excitable regime was described in Ref. [38].) This excitable dynamic is reminiscent of that found in Ref. [41] where a laser with a saturable absorber was considered using the Yamada model. Below threshold in the Yamada model, sufficiently strong perturbations can trigger a high-intensity pulse after which the system returns to the off state. The similarity with the behavior of the ES in our system is natural given the *Q*-switching-like behavior of our system. We note that while we require a master laser in our work, our slave device is somewhat simpler since the need for a saturable absorber is removed: The single section acts both as the amplifier and the gate for the pulses.

IV. CONCLUSION

In conclusion, we show experimentally and theoretically a form of type I excitability for an optically injected QD laser which differs from the classical mechanism described by the Adler equation for semiconductor lasers. The excitable response depends on the interplay of two lasing states operating in antiphase. While the underlying bifurcation structure of the excitation is of SNH form, there are several unique features in this system. The GS intensity undergoes a dropout featuring RO-like ringing while the ES displays antiphase short pulses. The excitable trajectory for the GS passes through a saddle focus which is responsible for the short ES pulses obtained. These short pulses have a technological potential for pulse reshaping and the production of tunable pulse trains. Further, while the SNH bifurcation is responsible for the generation of the excitable events, the phase trajectories are bounded, in contrast to all other instances of type I excitability in the optical injection system. It also provides another avenue for the study of neuromorphic systems using semiconductor lasers.

ACKNOWLEDGMENTS

E.A.V. acknowledges support from the Government of the Russian Federation (Grant No. 08-08). M.D. and B.K. thank Cleitus Antony and the Photonic Systems Group for use of equipment.

[1] A. L. Hodgkin and A. F. Huxley, J. Physiol. **117**, 500 (1952).
[2] J. M. Davidenko, A. V. Pertsov, R. Salomonsz, W. Baxter, and J. Jalife, Nature (London) **355**, 349 (1992).
[3] A. M. Zhabotinsky, Biofizika **9**, 306 (1964).
[4] A. Zhabotinsky and A. Zaikin, J. Theor. Biol. **40**, 45 (1973).
[5] T. S. Briggs and W. C. Rauscher, J. Chem. Educ. **50**, 496 (1973).
[6] S. Wieczorek, B. Krauskopf, and D. Lenstra, Phys. Rev. Lett. **88**, 063901 (2002).
[7] D. Goulding, S. P. Hegarty, O. Rasskazov, S. Melnik, M. Hartnett, G. Greene, J. G. McInerney, D. Rachinskii, and G. Huyet, Phys. Rev. Lett. **98**, 153903 (2007).
[8] B. Kelleher, C. Bonatto, G. Huyet, and S. P. Hegarty, Phys. Rev. E **83**, 026207 (2011).
[9] M. Giudici, C. Green, G. Giacomelli, U. Nespolo, and J. R. Tredicce, Phys. Rev. E **55**, 6414 (1997).
[10] F. Plaza, M. Velarde, F. Arecchi, S. Boccaletti, M. Ciofini, and R. Meucci, Europhys. Lett. **38**, 85 (1997).
[11] H. J. Wünsche, O. Brox, M. Radziunas, and F. Henneberger, Phys. Rev. Lett. **88**, 023901 (2001).
[12] A. M. Yacomotti, M. C. Eguia, J. Aliaga, O. E. Martinez, G. B. Mindlin, and A. Lipsich, Phys. Rev. Lett. **83**, 292 (1999).
[13] S. Beri, L. Mashall, L. Gelens, G. Van der Sande, G. Mezosi, M. Sorel, J. Danckaert, and G. Verschaffelt, Phys. Lett. A **374**, 739 (2010).
[14] P. R. Prucnal, B. J. Shastri, T. F. de Lima, M. A. Nahmias, and A. N. Tait, Adv. Opt. Photonics **8**, 228 (2016).
[15] B. J. Shastri, M. A. Nahmias, A. N. Tait, A. W. Rodriguez, B. Wu, and P. R. Prucnal, Sci. Rep. **6**, 19126 (2016).
[16] F. Selmi, R. Braive, G. Beaudoin, I. Sagnes, R. Kuszelewicz, T. Erneux, and S. Barbay, Phys. Rev. E **94**, 042219 (2016).
[17] S. Terrien, B. Krauskopf, N. G. R. Broderick, L. Andréoli, F. Selmi, R. Braive, G. Beaudoin, I. Sagnes, and S. Barbay, Phys. Rev. A **96**, 043863 (2017).
[18] B. Kelleher, B. Tykalewicz, D. Goulding, N. Fedorov, I. Dubinkin, T. Erneux, and E. A. Viktorov, Sci. Rep. **7**, 8414 (2017).
[19] J. Robertson, T. Deng, J. Javaloyes, and A. Hurtado, Opt. Lett. **42**, 1560 (2017).
[20] S. Wieczorek, B. Krauskopf, T. Simpson, and D. Lenstra, Phys. Rep. **416**, 1 (2005).
[21] T. Erneux and P. Glorieux, *Laser Dynamics* (Cambridge University Press, Cambridge, UK, 2010).
[22] B. Kelleher, D. Goulding, S. P. Hegarty, G. Huyet, D.-Y. Cong, A. Martinez, A. Lemaître, A. Ramdane, M. Fischer, F. Gerschütz *et al.*, Opt. Lett. **34**, 440 (2009).
[23] B. Lindner, J. Garćia-Ojalvo, A. Neiman, and L. Schimansky-Geier, Phys. Rep. **392**, 321 (2004).
[24] M. Turconi, B. Garbin, M. Feyereisen, M. Giudici, and S. Barland, Phys. Rev. E **88**, 022923 (2013).

[25] B. Garbin, D. Goulding, S. P. Hegarty, G. Huyet, B. Kelleher, and S. Barland, Opt. Lett. **39**, 1254 (2014).
[26] A. Markus, J. Chen, C. Paranthoen, A. Fiore, C. Platz, and O. Gauthier-Lafaye, Appl. Phys. Lett. **82**, 1818 (2003).
[27] M. Abusaa, J. Danckaert, E. A. Viktorov, and T. Erneux, Phys. Rev. A **87**, 063827 (2013).
[28] B. Kelleher, D. Goulding, S. Hegarty, G. Huyet, E. Viktorov, and T. Erneux, *Quantum Dot Devices* (Springer, Berlin, 2012), pp. 1–22.
[29] B. Lingnau, W. W. Chow, E. Schöll, and K. Lüdge, New J. Phys. **15**, 093031 (2013).
[30] A. Hurtado, I. D. Henning, M. J. Adams, and L. F. Lester, IEEE Photonics J. **5**, 5900107 (2013).
[31] B. Tykalewicz, D. Goulding, S. P. Hegarty, G. Huyet, D. Byrne, R. Phelan, and B. Kelleher, Opt. Lett. **39**, 4607 (2014).
[32] E. A. Viktorov, I. Dubinkin, N. Fedorov, T. Erneux, B. Tykalewicz, S. P. Hegarty, G. Huyet, D. Goulding, and B. Kelleher, Opt. Lett. **41**, 3555 (2016).
[33] C. Wang, B. Lingnau, K. Lüdge, J. Even, and F. Grillot, IEEE J. Quantum Electron. **50**, 1 (2014).
[34] R. Adler, Proc. IEEE **61**, 1380 (1973).
[35] B. Kelleher, D. Goulding, B. Baselga Pascual, S. P. Hegarty, and G. Huyet, Phys. Rev. E **85**, 046212 (2012).
[36] J. Thévenin, M. Romanelli, M. Vallet, M. Brunel, and T. Erneux, Phys. Rev. Lett. **107**, 104101 (2011).
[37] B. Kelleher, D. Goulding, B. Baselga Pascual, S. P. Hegarty, and G. Huyet, Eur. Phys. J. D **58**, 175 (2010).
[38] B. Tykalewicz, D. Goulding, S. P. Hegarty, G. Huyet, I. Dubinkin, N. Fedorov, T. Erneux, E. A. Viktorov, and B. Kelleher, Opt. Lett. **41**, 1034 (2016).
[39] B. Kelleher, C. Bonatto, P. Skoda, S. P. Hegarty, and G. Huyet, Phys. Rev. E **81**, 049901(E) (2010).
[40] B. Lingnau, K. Lüdge, W. W. Chow, and E. Schöll, Phys. Rev. E **86**, 065201(R) (2012).
[41] J. L. A. Dubbeldam, B. Krauskopf, and D. Lenstra, Phys. Rev. E **60**, 6580 (1999).